MASTER

IDO-16528

Reactors - General
TID-4500 (14th Ed.)

ANALYSIS OF SELF-SHUTDOWN BEHAVIOR IN THE SPERT I REACTOR

S. G. Forbes, F. L. Bentzen, P. French, J. E. Grund,
J. C. Haire, W. E. Nyer, and R. F. Walker

July 23, 1959

AEC RESEARCH AND DEVELOPMENT REPORT

PHILLIPS PETROLEUM CO.
ATOMIC ENERGY DIVISION
(UNDER CONTRACT NO. AT (10-1)-205)
IDAHO OPERATIONS OFFICE
U. S. ATOMIC ENERGY COMMISSION

PAGES 1 to 2

WERE INTENTIONALLY

LEFT BLANK

ANALYSIS OF SELF-SHUTDOWN BEHAVIOR IN THE SPERT I REACTOR *

by

S. G. Forbes, F. L. Bentzen, P. French, J. E. Grund,
J. C. Haire, W. E. Nyer, and R. F. Walker

A B S T R A C T

Experimental and theoretical work on the self-limiting response of reactors to step and ramp insertions of reactivity is discussed along with the general characteristics of self-limiting power bursts. The static characteristics of the cores investigated are presented and the techniques of measurement are discussed. Data from step and ramp tests are presented and compared with the predictions of a theoretical formulation of reactor self-shutdown in terms of energy release. The discussion includes an evaluation of some postulated shutdown mechanisms in the light of experimental results. Some results of detailed calculations of shutdown effects due to specific mechanisms which are believed to contribute significantly to reactor self-shutdown are presented.

---

* The material in this report was presented at the 1958 Winter Meeting of the American Nuclear Society,[1] December 9, 1958.

THIS PAGE

WAS INTENTIONALLY

LEFT BLANK

TABLE OF CONTENTS

LIST OF FIGURES

ANALYSIS OF SELF-SHUTDOWN BEHAVIOR IN THE SPERT I REACTOR

Introduction

This report presents some of the recent experimental and theoretical work on the self-limiting response of reactors to step and ramp injections of reactivity. For completeness, earlier work[2,3,18] is included. The experimental work includes information on four aluminum cores and a stainless steel core. The theoretical discussions present some results of a general formulation of self-shutdown effects in terms of the energy released by the reactor, and some results of detailed calculations of shutdown effects due to specific mechanisms.

By way of introduction to the discussion, it is desirable to point out some of the general characteristics of self-limiting reactor power bursts induced by the step injection of reactivity which are common to all the Spert I cores. Fig. 1 shows representative plots, on logarithmic scales, of relative values of the power, energy and compensated reactivity at the time of peak power as functions of the initial reciprocal period, α. All step-tests were initiated from low power levels.

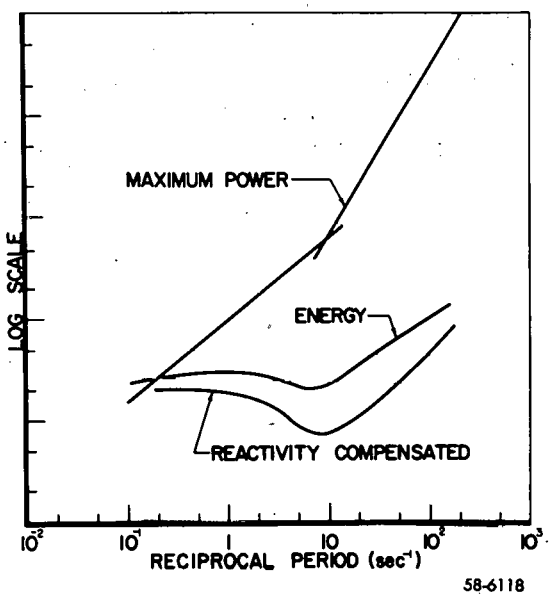

Fig. 1 - General Characteristics of Power Bursts

The peak power curve in the region of small α is approximately a straight line with slope about 1, and in the region of large α is approximately a straight line with slope nearly 2. There is a distinct break separating the two regions. The curves of reactivity compensated at the time of maximum power and the energy at the time of maximum power each show a distinct maximum and minimum. These minima and the break in the power curve are located at α approximately 7, which corresponds to a reactivity injection sufficient to make the reactor prompt critical. For α greater than about 7 the general behavior of these functions is largely in accordance with the predictions of a model for burst behavior first used by Fuchs[4,5] in which the loss of reactivity arising from the energy release is assumed to be proportional to the energy release. That is, the equation coupling reactivity changes with the power history has the form

$$\alpha(t) = \alpha_0 - b\,E(t) \qquad (1)$$

where α_0 is the initial reciprocal period, $E(t)$ is the energy release

at time t and b is the shutdown coefficient. The general features of the experimental curves in the region below α about 7 are also exhibited by machine calculations based on this model when delayed neutrons are taken into account(6). It can be shown (7) that these features are related to the shape of the burst. A burst similar to that of the Fuchs model shows a distinct maximum and minimum in the reactivity compensation at the time of peak power as a function of the reciprocal period, α, and a break in the peak power versus α curve. In the limit of very broad or very narrow bursts these features disappear(8). Whether the power burst shape of a particular reactor is broad or narrow is determined by the abruptness with which reactivity changes occur during a transient. To the extent that the detailed nature of the shutdown process can be inferred from the abruptness with which they take place, the summary curves of reactivity compensation and power at the time of peak do provide at least qualitative information regarding the general characteristics of the self-limiting process.

An important feature of the Fuchs model is that bursts are characterized by only two parameters, the reciprocal period, α, and the reactivity coefficient of the core. For this model the vertical scales for the power and energy functions displayed in the figure vary linearly with the reactivity coefficient. This report describes tests with cores of different reactivity coefficients originally undertaken for the purpose of checking this prediction.

Empirical Model for Burst Behavior

In several important ways the Fuchs model failed to agree with the early experimental data. For example, the predicted burst shape was noticeably different from the observed shape. Analytical work was undertaken to modify the theory to fit the burst behavior in more detail[9] with the view that if a good match could be obtained between the experimental and calculated power behavior, the requisite form for the coupling equation could then be investigated for possible physical significance.

Since some of the features of the experimental data suggest a general form for the coupling equation in which there is a time delay between the energy released by fission and the appearance of reactivity changes, and that this reactivity change is a non-linear function of the delayed energy, these features were incorporated into the prompt kinetics equations which can then be expressed as follows:

$$\frac{\dot{\phi}}{\phi} = \alpha_0 - b\left[E(t-\tau)\right]^n \qquad (2)$$

$$\tau = 0, \qquad \text{Zero Delay}$$

$$\tau \gg 1/\alpha_0, \qquad \text{Long Delay}$$

in which E denotes the energy produced by the reactor from the start of the transient up to the time t minus τ where τ is the delay time between energy release and its manifestation as shutdown effect. ϕ is the reactor power, $\dot{\phi}$ is its time derivative, and α_0 is the reciprocal of the initial asymptotic period following a step increase in the reactivity. n is a positive constant, and b is a constant proportional to the reactivity change produced by the energy in the shutdown mechanism. The mechanism is not specified, but may be identified from physical considerations in some reactor systems.

This equation has been solved for both $\tau = 0$ and τ much greater than the initial asymptotic period $1/\alpha_0$. For the zero-delay case, E becomes simply the integral of the power up to the time, t, while for the long-delay case E becomes the integral of the early part of the power rise, thus E^n is a simple exponential with an exponent n times that of the initial power rise. For n = 1 and $\tau = 0$, Eq. (2) reduces to the Fuchs model Eq. (1).

It is found that by appropriate choice of the constant n, either the zero-delay or long-delay solutions will provide an adequate fit to the experimental power burst up to the time of peak. However, the long-delay form is required to match the post-peak behavior. This is illustrated in Figs. 2 and 3, where the log of the power is shown on the ordinate and time from peak in periods is shown on the abscissa.

In Fig. 2, the solid lines are the analytical results from the zero delay model for different values of the constant n, and the points are experimental data from a 9.5 msec transient. Up to the time of peak the experimental burst is matched rather well by the n = 2 curve, but the post-peak agreement is poor. It should be noted that the zero-delay case with n = 1, the simple Fuchs model, which has been

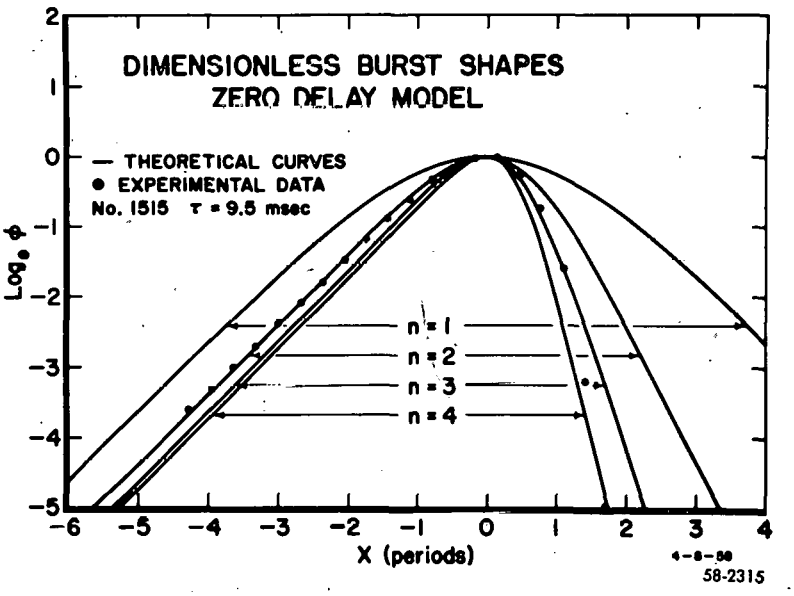

Fig. 2

shown to predict many of the general features of burst behavior, does not represent the power burst well in the short-period region. In fact, it can be stated that a simple shutdown proportional to the energy release will not match the experimentally observed power behavior for either zero-delay or long-delay models, and that a non-linear relationship must be used; that is, n must be significantly greater than unity. In the limit of large n it can be shown[8] that both the compensated reactivity at the time of peak power and the peak power itself are linear functions of α for all α, even in the delayed neutron region. In Fig. 3 the same experimental burst is compared with results from the long-delay model. For n = 1.5 the agreement is good, not only for the rising part of the curve, but also on the falling side, for at least two decades below the peak. The curve for large n approaches an "exponential sawtooth", as indicated by the case for n = 100.

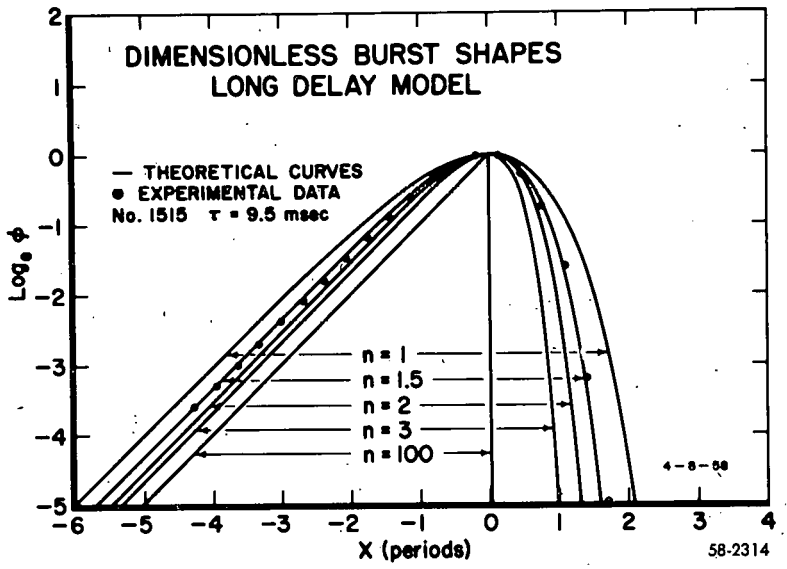

Fig. 3

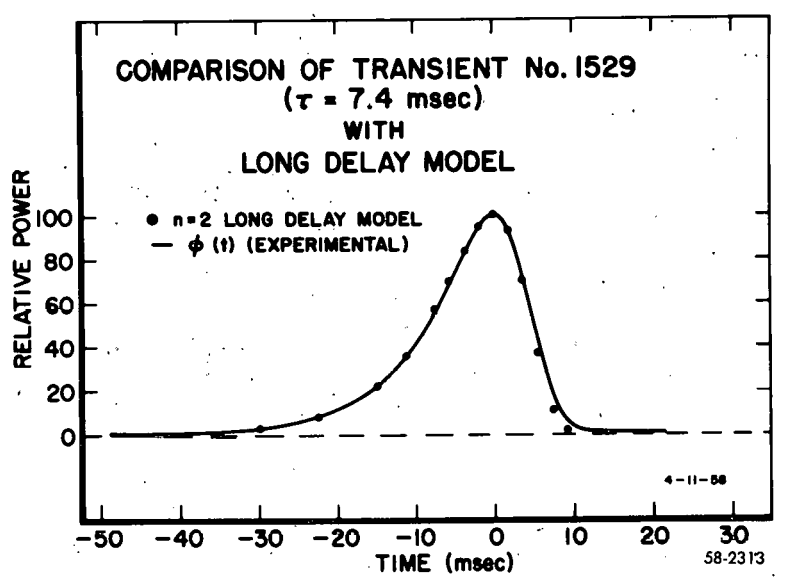

Fig. 4

In Fig. 4 the observed power shape for a 7.4 msec transient is compared with the long-delay model with n = 2 on a linear scale. The solid line was traced directly from the oscillograph record. The agreement is good except for a small deviation near the tail.

Another point of comparison between the model and experiment is the reactivity behavior as a function of time during a burst. In Fig. 5, the experimental values of reactivity compensation as a function of time are shown for a 9.5 msec transient. The compensated reactivity was

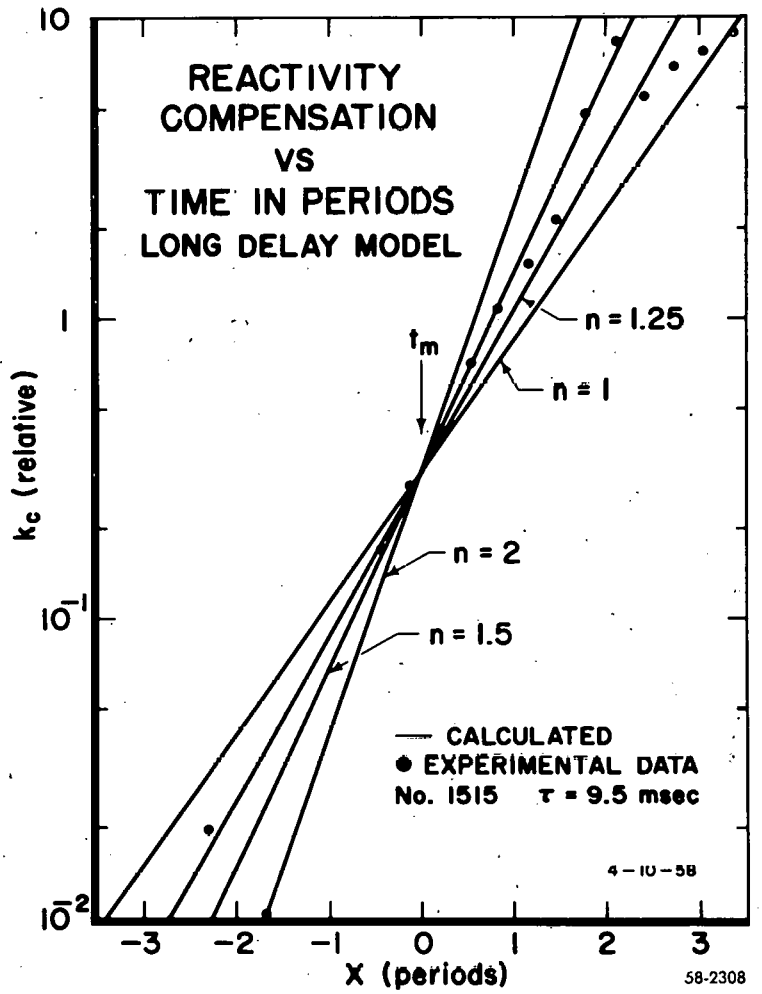

Fig. 5

obtained by analysis of the experimental power burst using the reactor kinetics equations[10]. The calculated lines are for different values of n in the long-delay model. It is seen that for one to two periods on either side of the power peak, the reactivity compensation is growing exponentially with an exponent about one-and-a-half times greater than that of the initial power rise. That is, of course, exactly the form of the long-delay model, where the ratio was expressed as the constant n, and n was found to be between 1.5 and 2.0 for the best fit to the power data. The same general behavior is exhibited by all the short-period, sub-cooled step transients.

A result of particular interest is the prediction of the dependence of the reactor peak power, $\phi(t_m)$, on the parameters a, b and n. The analytical results are given in Eqs. (3) and (4) for the zero-delay and long-delay cases, respectively.

$$\phi(t_m) = \frac{\alpha^{\frac{n+1}{n}}}{b^{1/n}} \left(\frac{n+1}{n} \right) \qquad \text{Zero Delay} \qquad (3)$$

$$\phi(t_m) = \frac{\alpha^{\frac{n+1}{n}}}{b^{1/n}} \left(e^{\alpha\tau} - 1/n \right) \qquad \text{Long Delay} \qquad (4)$$

In each case, the same dependence on α appears with an additional dependence on the product, $\alpha\tau$, appearing in the long-delay case. In both cases, the peak power is seen to be proportional to the reciprocal of the nth root of the shutdown coefficient, b. Since n is found to be of the order of two, this implies that the dependence on the constant b, which is proportional to the ratio of the void coefficient to the prompt neutron lifetime, is weaker than the linear dependence predicted from the simple Fuchs model. Therefore, for similar reactors it would be expected that the peak power would vary approximately as the reciprocal of the square root of the void coefficient over the lifetime. This weakened dependence on b is implicit in any reactor which displays a shutdown effect that increases more rapidly than the energy released, and is not therefore unique to the analytical form used here.

Static Characteristics of Spert I Cores

The experimental techniques for determining the static characteristics of the cores used in the study of the effect of the shutdown coefficient on kinetic behavior, and the results of the measurements[11] are presented in this section.

Fig. 6 is a cut-away view of the reactor vessel in which these tests have been conducted.

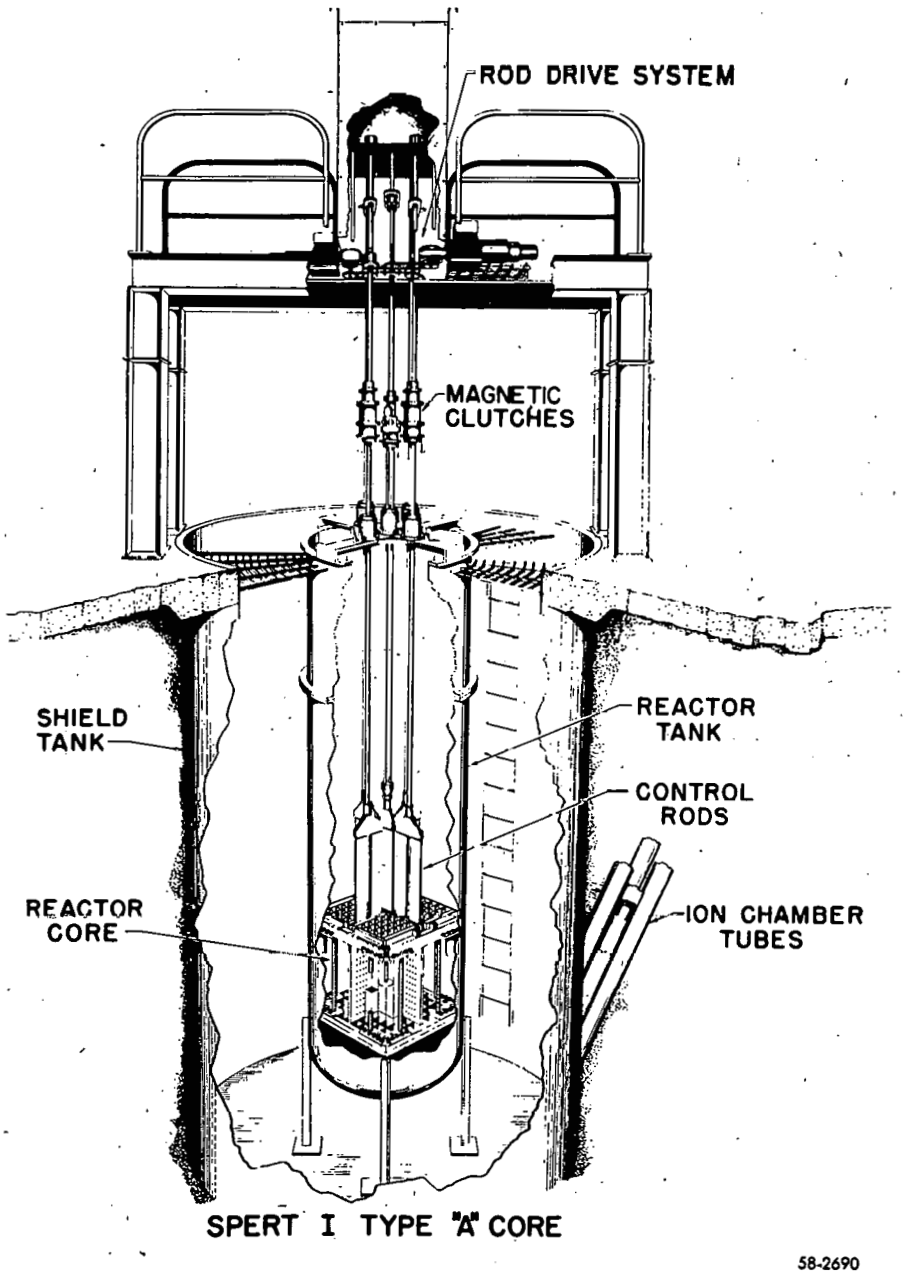

Fig. 6 - Spert I - Reactor Cutaway

The Spert I cores are contained in the open tank four feet in diameter and fifteen feet high. This tank is normally filled to a point about two feet above the core with light water which serves as a moderator and reflector. The internal structure shown is that used for the first four cores, which were of aluminum construction. This structure has been modified for the stainless steel core presently under investigation.

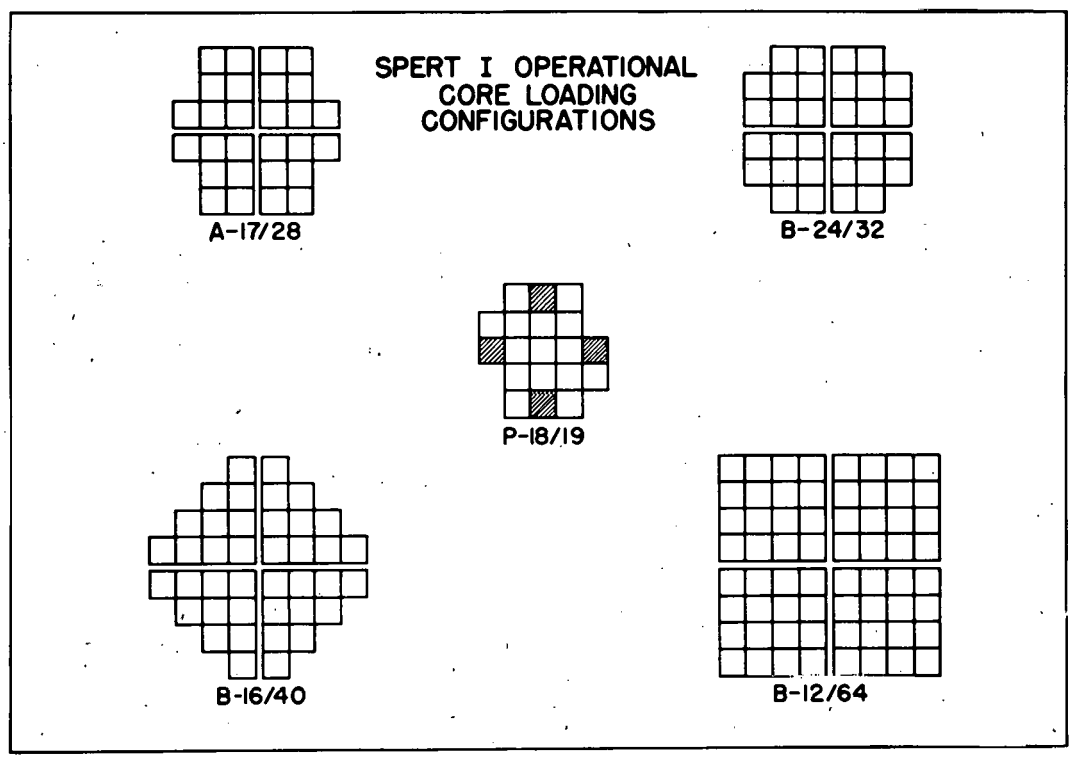

Fig. 7

Illustrated in Fig. 7 are plan views of the operational loadings for the five cores used in transient tests. The cores are designated by a letter for the type fuel assembly used. The first number denotes the number of fuel plates per assembly and the second number is the number of fuel assemblies in the operational core. Since all the cores are approximately the same height, the core volumes are proportional to the plan view areas shown. The core volumes, in fact, differ by nearly a factor of four between the P-18/19 core and the B-12/64 core.

The A core was made up of Type "A" fuel assemblies which were plate-type, box-form aluminum assemblies with nominal dimensions of 3 in. by 3 in. by 24 in. long. Each assembly had 17 fixed fuel plates separated by 117 mil water channels. The fuel plates consisted of a 20 mil enriched uranium-aluminum alloy meat, clad with 20 mil aluminum.

The B cores were composed of assemblies that were essentially identical to the Type "A" assemblies, except that they had four permanently brazed-in fuel plates and 20 removable fuel plates. This permitted variation in the number of plates per assembly and consequently, variation of the water moderator channel thickness between plates. These alterations were to provide sizable changes in the void coefficients while leaving other static characteristics relatively unchanged.

Three Type "B" assembly configurations were used for the static tests and subsequent transient tests. These were:

(1) The B-24 assembly with 24 fuel plates per assembly and 65 mil water channels used in the B-24 core;

(2) The B-16 assembly with 16 fuel plates per assembly and alternate 190 and 65 mil water channels used in the B-16 core; and,

(3) The B-12 assembly with 12 fuel plates per assembly and 190 mil water channels used in the B-12 core.

Blade-type control rods, which were located in the control rod guide structure that divided the core into quadrants, were used for all the aluminum cores.

The core presently under investigation, the P-18/19 core, is composed of stainless steel APPR-type fuel assemblies. These fuel assemblies are box-form with nominal dimensions 3 in. square by 22 in. long. Each assembly has 18 fuel plates, each plate consisting of a 20 mil uranium oxide-stainless steel meat, clad with 5 mil 304L stainless steel. The water channel between plates is 133 mils. The shaded areas in the plan view are the fuel-poison control rods used with this core.

Fig. 8 shows a plot of critical mass versus hydrogen-to-uranium ratio for the five cores investigated. The hydrogen-to-uranium ratio differs by a factor of six between the P core, on the left, and the B-12 core, on the right, with the other cores having intermediate values. The B-16 core was near the minimum critical mass achievable with this configuration.

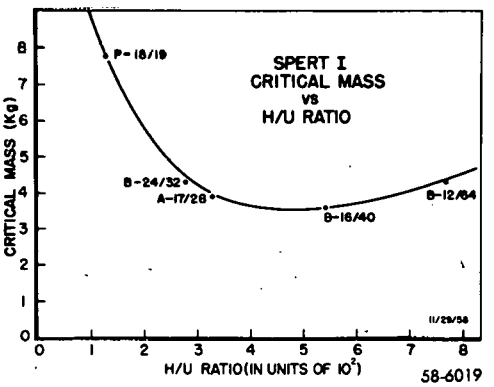

Fig. 8

The excess reactivity in each operational core was of the order of four to six dollars, which was sufficient to conduct the transient test series. The excess reactivity was determined from control rod calibrations by the period method using boric acid as a distributed poison.

Flux distributions in each core were obtained by gold foil activation.

Temperature effects were determined by heating the water in the reactor tank from ambient temperatures to boiling with electrical heaters. Reactivity changes and a temperature coefficient were obtained from this temperature range. The temperature coefficient differs by a factor of nearly six among the cores at 20°C, but the total temperature defect between ambient and boiling was nearly constant for all the cores. This temperature defect between ambient and boiling ranged from one dollar forty cents to one dollar seventy cents reactivity for all the cores.

As stated above, the purpose of the B cores was to effect sizable changes in the void coefficient and to determine its effect on the system's dynamic behavior. Several experimental devices, such as styrofoam sheets, plastic air bags, aluminum and magnesium plates, and a sealed fuel assembly were used to simulate voids in the water moderator. These devices were for the purpose of evaluating the reactivity effects of distributed and localized voids. Experiments were conducted to determine the interaction effects of voids in various core locations and the combined effects of voids and temperature.

The average void coefficient was found to be negative in all cases. As is shown in Table I, this coefficient varied by a factor of nearly ten among the cores with the B-12 core having the smallest value, and the P core having the largest. The local void coefficient was also negative for all except the B-12 core, where a positive coefficient was found near the center of the core.

The experimentally determined ratio of the effective neutron lifetime, ℓ^*, to effective delayed neutron fraction, $\bar{\beta}$, is also shown.

The ratio of these two experimentally determined quantities, c_v, the average void coefficient in dollars per cubic centimeter, and $\ell^*/\bar{\beta}$, is c_v/ℓ^*, in % $\Delta k/cm^3$-sec. It is shown in the bottom row and is proportional to b, the reactivity coefficient. It increases from the minimum value of 0.9 for the B-12 core through the values for the B-16, A, and B-24 cores to a maximum of 50 for the P core.

The five cores differ in several features, but the main one is the factor of fifty difference in the c_v/ℓ^* ratio and the order in which it increases. It is the effect of this parameter on the transient behavior that is to be compared with the predictions of the models.

TABLE I

Static Characteristics of the Spert I Core

Core	B-12/64	B-16/40	A-17/28	3-24/32	P-18/19
Clad Material	Al	Al	Al	Al	SS
Critical Mass, Kg U-235	4.3	3.6	3.9	4.3	7.6
Total U-235 Loaded, Kg	5.4	4.5	4.7	5.4	9.3
H/U Ratio	760	540	320	270	120
M/W Ratio	0.46	0.63	0.79	1.14	0.3
Available Excess Reactivity, $	4.3	5.6	5.2	6.6	4.9
Temperature Defect, 20° - 95°C, $	1.44	1.67	1.47	1.73	1.48
Temperature Coefficient, 20°C, $/$^{\circ}$C	-1.8×10^{-2}	-1.7×10^{-2}	-0.67×10^{-2}	-1.1×10^{-2}	-0.25×10^{-2}
Temperature Coefficient 95°C, $/$^{\circ}$C	-2.0×10^{-2}	-3.4×10^{-2}	-2.7×10^{-2}	-3.4×10^{-2}	-3.4×10^{-2}
Central Void Coefficient, $/cm^3	$+0.8 \times 10^{-4}$	-4.7×10^{-4}	-9.3×10^{-4}	-17×10^{-4}	-18×10^{-4}
Average Void Coefficient, c_v, $/cm^3	-0.93×10^{-4}	-2.9×10^{-4}	-4.6×10^{-4}	-7.3×10^{-4}	-9.9×10^{-4}
$\ell^*/\bar{\beta}$ (sec)	11×10^{-3}	10×10^{-3}	7×10^{-3}	7×10^{-3}	2×10^{-3}
$\frac{c_v/\bar{\beta}}{\ell^*/\bar{\beta}}$ (% $\Delta k/cm^3$-sec)	0.9	3	7	10	50

Dynamic Behavior - Step Tests

The generality of the shutdown model Eq. (2) makes it applicable to many reactors, but on the other hand, does not predict the detailed dependence of kinetic behavior on specific shutdown mechanisms. However, Eq. (2) can be interpreted as specifically including the shutdown coefficient in the constant b. Thus it gives a quantitative prediction of the dependence of kinetic behavior on this quantity, which is believed to be significant on the basis of general considerations. A reactor with a large negative void coefficient would be expected to shut down with a smaller energy release than one with a small negative void coefficient. Five cores with widely differing shutdown coefficients have been used to determine this dependence experimentally, and the results have been compared with the predictions from theory.

In Fig. 9 are shown the general features of the data from a transient with an asymptotic period of 17 msec, which corresponds to an α of approximately 60. This is typical of all short period step transients and indicates the general behavior of the variables on arbitrary scales as a function of time. The most useful index of the dynamic reactor behavior is the power. Since it often rises nine or more decades, (from below one watt to greater than 10^9 watts), it is usually plotted on a logarithmic scale as shown. The shape of the burst is also important because, as mentioned above, a sharp turnover implies a weak dependence on the shutdown coefficient, b, in contrast with a round top burst which implies a stronger dependence on b. The reactivity of the system, shown near the center of the figure, is calculated from the power history. Only a small change in reactivity is necessary to stop the rise, but a much greater negative reactivity develops later. The fact that most of the reactivity change occurs after the energy release by fission is essentially complete indicates a delay between the energy release and the appearance of energy in the shutdown mechanism.

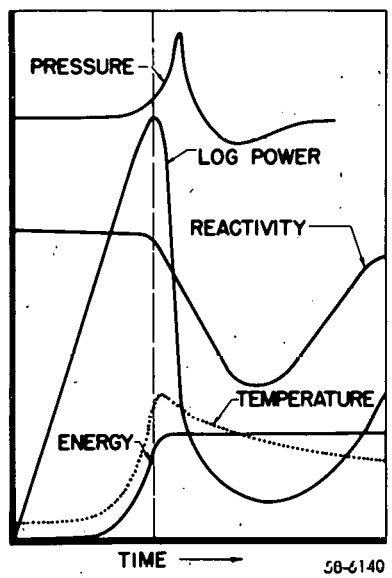

Fig. 9 - General Behavior of Parameters During Transient

For the shorter period transients about two-thirds of the total energy in the burst is released by the time of peak power. The energy is stored mainly in the fuel plates, causing the temperature rise as shown. The surface temperature of the plates at the time of peak power is the significant quantity in shutdown considerations. It is seen to be less than the maximum temperature which is reached after the power peak. The maximum temperature can be quite large and approaches the melting point of the fuel plates on the shortest period transients.

Transient pressure is another variable of importance in reactor safety. It is usually of sufficient magnitude to be measurable only on periods shorter than 35 msec, and has never been observed to exceed 100 psi in the end box, even for the shortest transients. The delay of the pressure peak with respect to the power peak is reduced as the period becomes shorter.

Summary data of the type just discussed for more than 200 step transients with initial asymptotic periods ranging from 20 sec to 5 msec, $\alpha \approx 0.05$ sec^{-1} to $\alpha \approx 200$ sec^{-1}, are shown in Figs. 10 through 14.

Fig. 10 shows the pressure measured in the end box of one of the central fuel assemblies for the five different cores. The pressure becomes observable only for large values of α. The scale for the abscissa matches that used for the temperature, power and energy functions in Figs. 11 through 13, and was selected to emphasize the small range of tests in which measurable pressures occurred. The experimental data show large scatter and straight-line fits are shown for comparison. It can be seen that the pressures are all small, and that the behavior is similar for all cores.

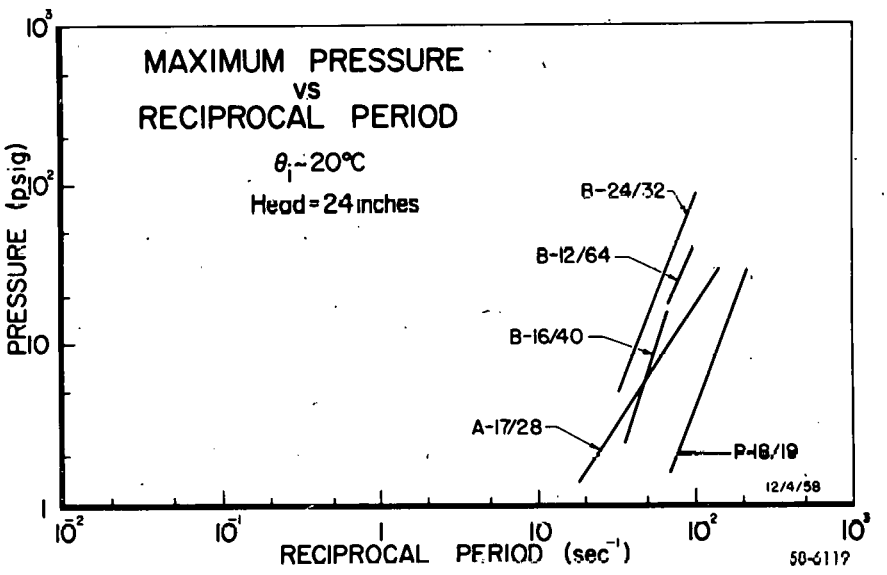

Fig. 10

Fig. 11 shows the maximum surface temperature as a function of α and the fuel plate surface temperature rise at the time of maximum power versus α.

The lower group of curves represents the surface temperature rise at peak power, which is the quantity of concern in heat transfer and reactor shutdown considerations. The dashed line at saturation

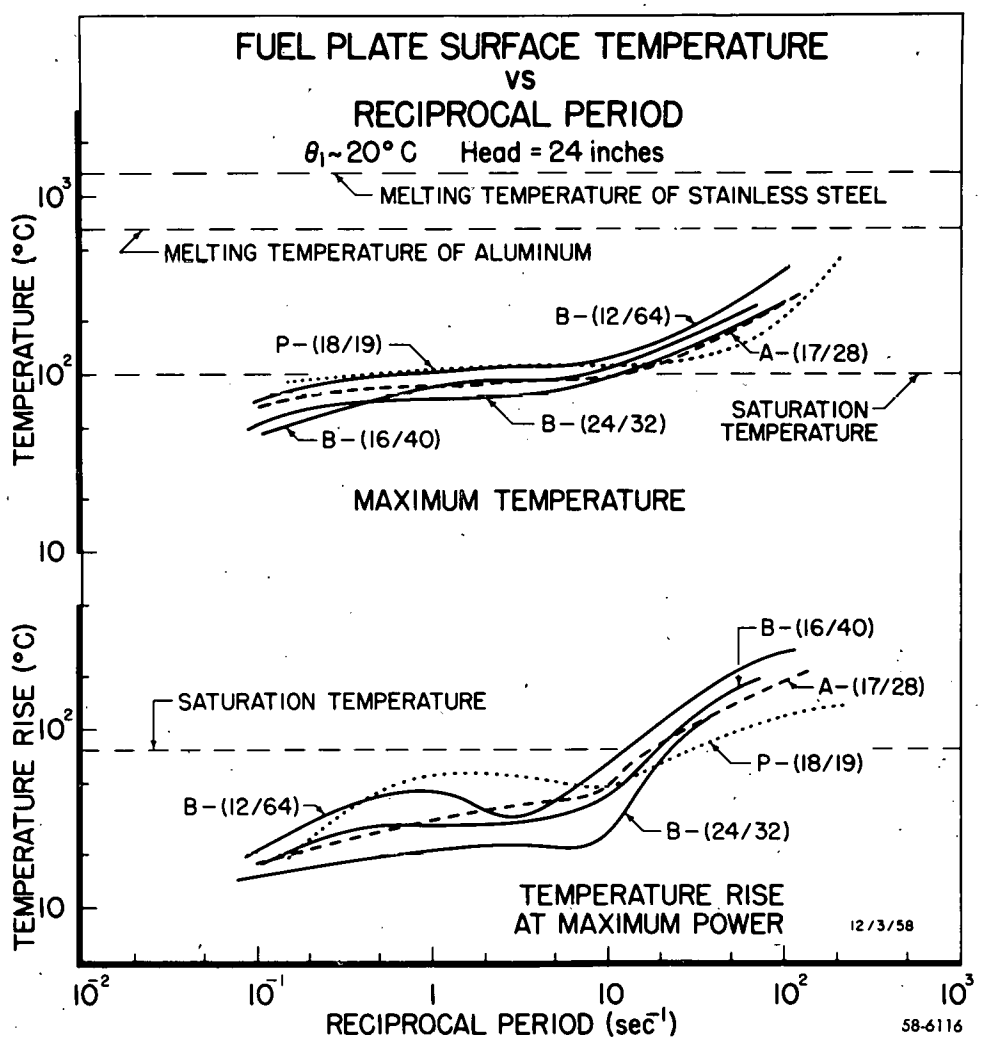

Fig. 11

temperature indicates that only for α larger than 10 does the fuel plate surface temperature exceed the boiling point of water. Therefore, some mechanism other than steam formation is required to explain the self-shutdown effect at long periods.

The upper group represents the maximum surface temperature. The values for a particular α all lie within a factor of two of each other, and in the large α region the B-12/64 core (the core with the smallest void coefficient and longest lifetime) reaches the highest temperature, while the P-18/19 core has the lowest temperature. It is apparent that periods slightly shorter than those already performed on these cores would result in temperatures exceeding the melting point of the fuel plates, as represented by the upper dashed lines.

Fig. 12 is a plot of the peak power reached during the burst for transients with different asymptotic periods. The two features which stand out are the remarkable similarity of the curves and the break between $\alpha = 5$ and 10. The lines to the left of the break have a slope slightly less than one, and the lines to the right of the break a slope of approximately two. The break can be shown to be a property of the burst shape and exists only for bursts that are not extremely sharp.

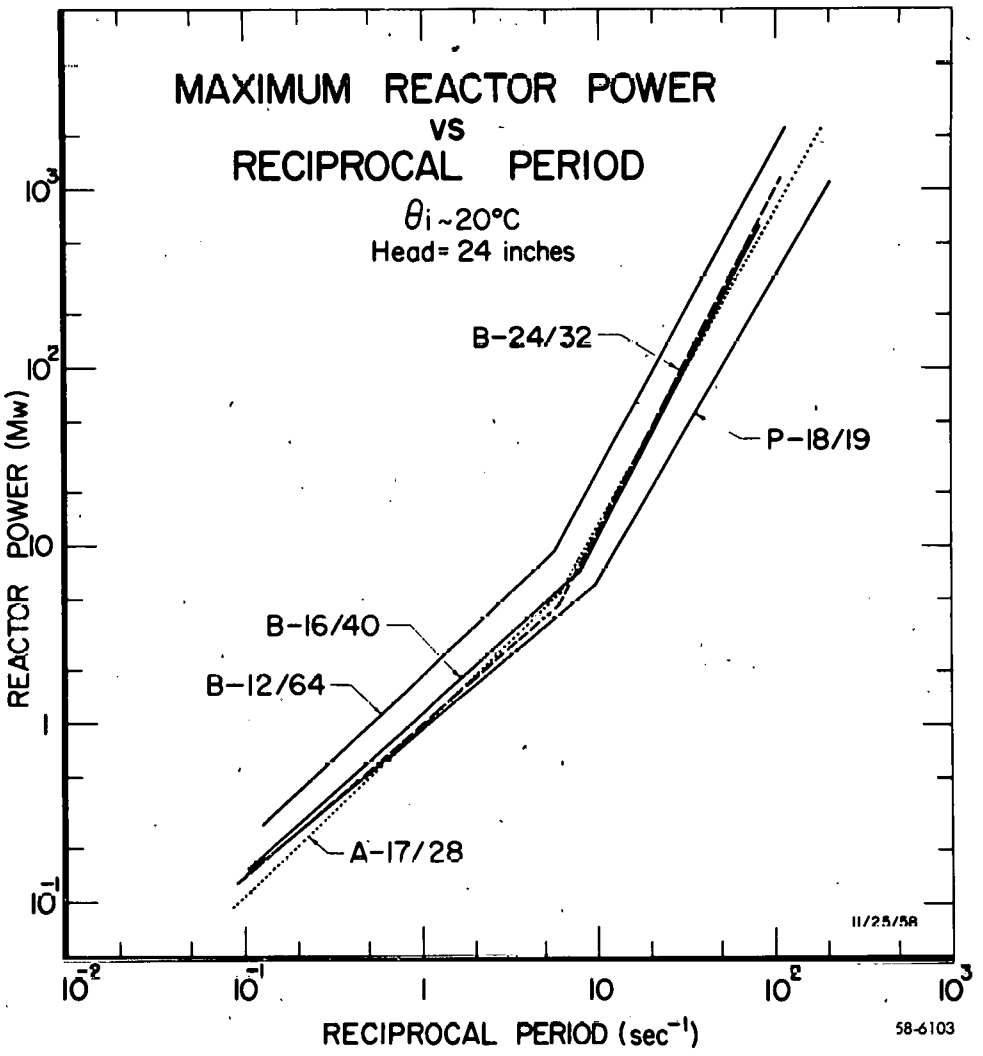

Fig. 12

In the prompt region the model predicts that the peak power for a given α should vary approximately as the reciprocal of the square root of the shutdown coefficient, b. Since b, which includes the void coefficient divided by the lifetime, has been shown to vary over a factor of 50, the estimated range for the peak powers is approximately 7.

The data show that 5.5 is the maximum spread for an α of 100. This is rather good agreement and indicates that the weak dependence on the shutdown coefficient predicted by the model does exist. The P-18/19 (stainless steel) core has the largest void coefficient and the shortest lifetime. This results in the smallest peak power for a particular α. The highest power occurs for the B-12/64 core, the one with the smallest void coefficient and the longest lifetime. The weakened dependence on the void coefficient lessens the reactor designer's control over dynamic characteristics through this parameter.

The energy released to the time of peak power is shown in Fig. 13. Energy release is measured primarily by integration of the power trace. The total energy can also be measured by bulk reactor temperature rise, and the two methods give results which agree to within 10%.

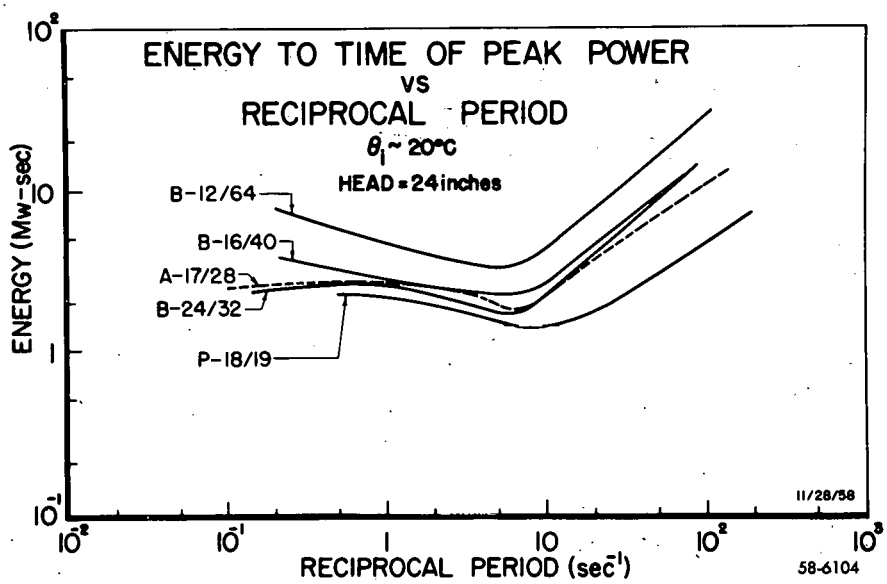

Fig. 13

The energy to maximum power, which is roughly two-thirds the total energy under the burst, exceeds 10 Mw-sec only for short periods. The uppermost line represents the B-12/64 core, which has the smallest void coefficient and the longest neutron lifetime, and the lowest curve represents the P-18/19 core with the largest void coefficient and shortest lifetime.

All the summary data so far presented have been plotted against α as the independent variable. This is a particularly useful index because it is experimentally observable, and in heat transfer and other considerations, it is the actual power rise or the rate of energy deposition that is of interest in correlation among cores. However, it should be emphasized that care must be taken when correlating cores on the basis of α because the implicit dependence on reactivity and lifetime may be obscured. For example, the peak power has been shown to

decrease for shorter lifetimes when compared on the basis of α. This is not the case when the correlations are made on the basis of reactivity. Here, as expected, the peak power is increased as the lifetime is shortened. It is not usually the power, however, but the energy released that is important in safety considerations, and Fig. 14 shows the energy to the peak power as a function of the reactivity in dollars. Curves of all the cores are quite similar, each having a distinct minimum near the prompt critical value of one dollar.

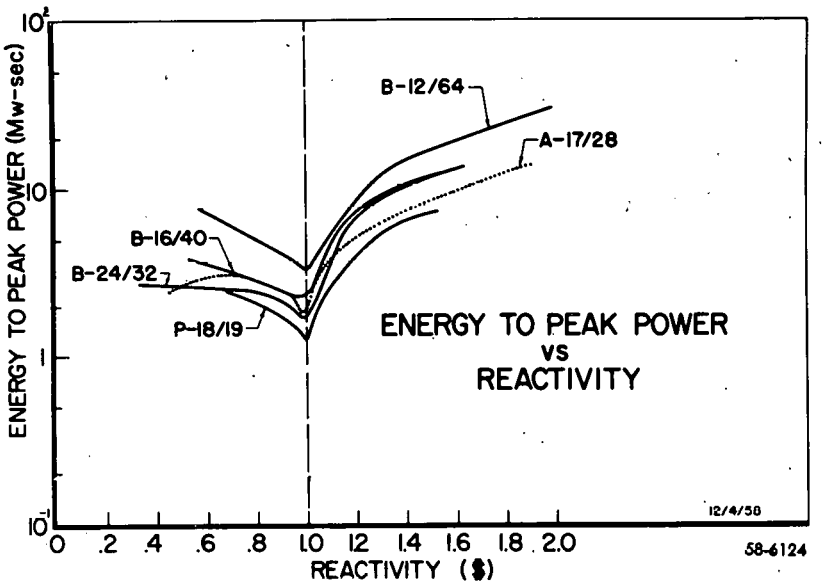

Fig. 14

For reactivity additions of one-and-one-half dollars, the energy release is approximately four times larger for the B-12/64 core than for the P-18/19 core with its large void coefficient and short neutron lifetime. Since the effective delayed neutron fraction, $\bar{\beta}$, is different for each core, these curves will be shifted slightly when delta k, rather than dollars, is used as the independent variable.

In summarizing the transient behavior of the Sport cores following a step addition of reactivity, the important results can be stated as follows: first, the behavior of all cores on the basis of α is remarkably similar, notwithstanding the inclusion of both aluminum and stainless steel cores and the wide range of static characteristics involved; and second, those changes that do exist are predicted by an elementary theory which incorporates two experimentally determined quantities--the average void coefficient and the neutron lifetime. The power- or energy-ratio at a constant α has been shown to vary inversely as the square root of the void coefficient, divided by the neutron lifetime. Also, on the basis of reactivity, increasing the void coefficient will result in a core that releases less energy.

Dynamic Behavior of the Spert Cores - Ramp Tests

In addition to the problems of reactor safety represented by the step tests, there is another group of problems which can be represented by the ramp-rate tests. In contrast with the step tests, the reactivity input increases continuously throughout the ramp experiment. Studies have been made on two cores to determine the response of the reactor to such disturbances.

Fig. 15 shows data obtained on the B-12/64 core. The initial temperature of 20°C and the water head, 24 inches above the core, were constants for all of the experimental results discussed in this section. Logarithmic reactor power versus time after initiation of the ramp is presented for various starting powers. Reactivity additions were begun with the reactor at delayed critical.

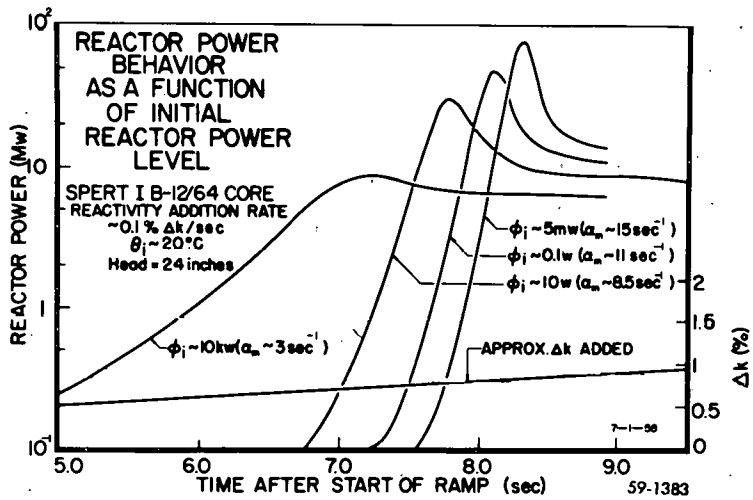

Fig. 15

In general, the reactor behavior following the initiation of a ramp reactivity insertion displays a rise in log power with slope increasing to a maximum and then decreasing to zero at the time of a power maximum. The area of principal concern in analyzing the ramp-rate data is the region of the power excursion up to and including the power maximum.

Two interesting parameters in ramp-induced excursions are the starting power and the reactivity addition rate, variations of both initial power and ramp-rate were therefore undertaken. The effect of starting power, denoted ϕ_i, on the reactor power behavior during an excursion can be seen in this figure.

The reactivity addition rate of approximately 0.1% Δk/sec was the same for all tests, and the reactivity addition is indicated by

the lower line in the figure. The peak power and the maximum reciprocal period, denoted α_m, are both observed to increase with decreasing initial power. However, the increase in peak power from the lowest to the highest was only about a factor of 10, from approximately 8 Mw and α_m of 3 reciprocal seconds to about 80 Mw and α_m of 15 reciprocal seconds, while the starting power decreased six decades from 10 kw to about 5 mw. Results of a similar nature were obtained on both cores and for all reactivity addition rates. The rate used for these tests, about 0.1% Δk/sec, is approximately the middle of the range of rates investigated which was from 0.01% to 0.3% Δk/sec.

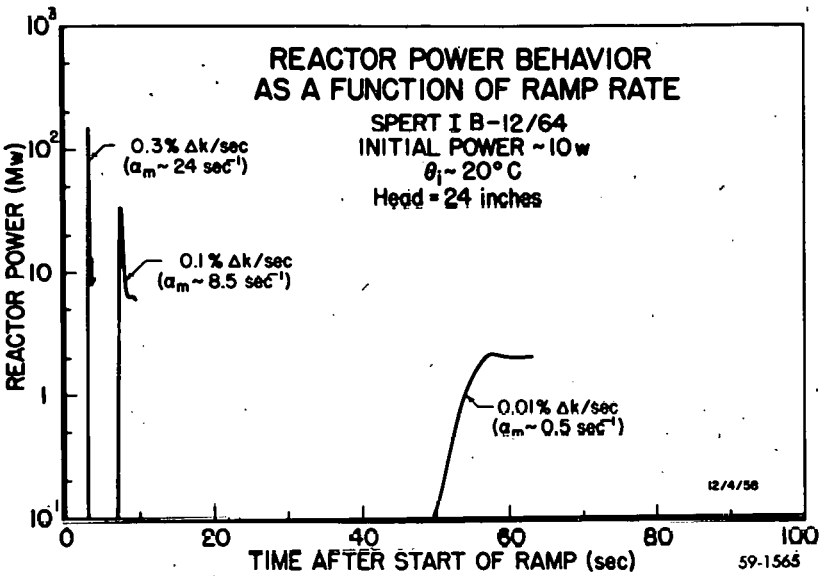

Fig. 16

The effect of ramp rate on the general behavior is illustrated in Fig. 16, which displays logarithmic reactor power versus time after initiation of the ramp as functions of ramp-rate with initial power held constant. These data are also from the B-12/64 core. The peak reactor power and the maximum reciprocal period are both observed to increase with increasing ramp rate. The peak power increased by a factor of approximately 100 from about 2 Mw to about 200 Mw; α increased from 0.5 reciprocal seconds to 24 reciprocal seconds; and the ramp rate increased by a factor of about 25, from 0.01% Δk/sec to 0.27% Δk/sec. Thus, an increase in the ramp rate is accompanied by an earlier power excursion with a larger reciprocal period and a higher maximum power. The starting power for the tests shown here was approximately ten watts and is about the mid-point of the nine decade range of starting powers investigated. The lowest was 10^{-4} w and the highest 10^{6} w. This behavior is representative of the behavior of both cores at all values of initial reactor power.

In Fig. 17 the maximum reactor power versus maximum reciprocal period data for ramp tests on the B-12/64 core is shown by the points. The solid line indicates step test data from the same core. The crosses, circles and triangles denote data for ramp rates of 0.01% Δk/sec; 0.1% Δk/sec; and 0.3% Δk/sec, respectively. The similarity

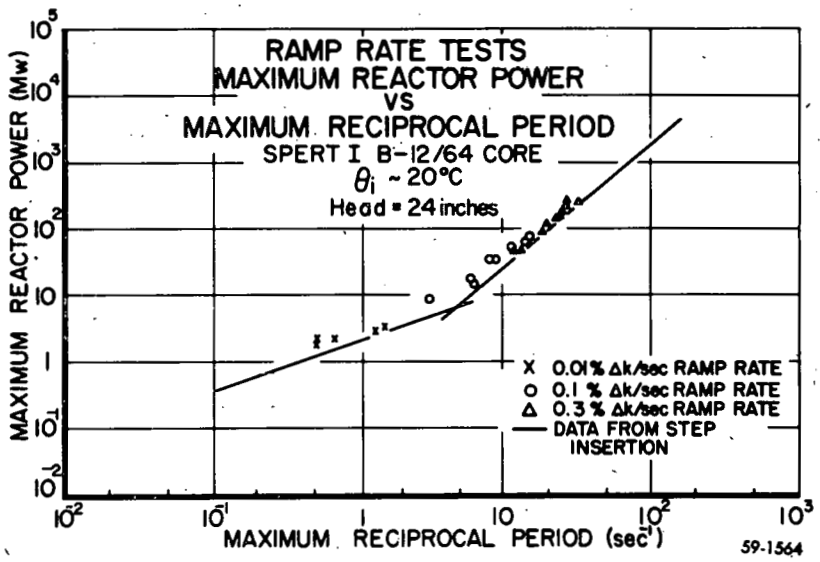

Fig. 17

between step and ramp data shows that the primary burst during a ramp induced excursion is essentially equivalent to a step excursion with initial reciprocal period equal to the maximum reciprocal period observed during the ramp burst. That is, if a ramp test is characterized by its maximum reciprocal period, it can be treated as a step test having equal initial reciprocal period. These general characteristics are the same as had been noted for the A core[2].

The observed characteristics of ramp induced excursions are predicted by the prompt kinetic equation, Eq. (1), with a modification to take into account the continuous addition of reactivity. The prompt equation for ramps then becomes

$$\alpha(t) = at - bE(t) \tag{5}$$

where $\tau = 0$, $n = 1$, and a, the only symbol not previous defined, is proportional to the rate of addition of reactivity.

The logarithmic derivative of the power with respect to time is defined as the reciprocal period, $\alpha(t)$

$$\frac{\dot{\phi}(t)}{\phi(t)} = \alpha(t). \tag{6}$$

From Eqs. (5) and (6), the reactor power, ϕ_m, at the time of the maximum reciprocal period may be shown to be[12]

$$\phi_m = \frac{a}{b} , \tag{7}$$

which is dependent solely on the ramp rate, a, and the reactivity coefficient, b. It is independent of the initial reactor power and also independent of the lifetime.

Also, the maximum power, ϕ_M, achieved during a ramp induced excursion is

$$\phi_M = \frac{a}{b} \ln \frac{\phi_M}{\phi_i} , \tag{8}$$

and the maximum reciprocal period, α_m, is given by

$$\alpha_m = \left[2a \left(\ln \frac{a}{b\phi_i} - 1 \right) \right]^{1/2} . \tag{9}$$

Thus, a weak dependence of α_m on initial power, ϕ_i, and reactivity coefficient, b, is predicted by this model. The strongest dependence is on the reactivity addition rate, a. Neglecting shutdown effects in Eq. (5), that is, setting $\alpha = at$ in Eq. (6), would lead to a reciprocal period,

$$\alpha = \left[2a \ \ln \frac{a}{b\phi_i} \right]^{1/2} \tag{10}$$

at the power $\phi_m = a/b$. This α differs very little from that given by Eq. (9). Thus the reactor behaves largely as if there were no shutdown effects up to the power given by Eq. (7). That is, the reactivity up to this power is essentially the term at.

The maximum power in a ramp burst can be shown to also take the form,

$$\phi_M = \frac{\alpha_m^2}{2b} \frac{\ln \frac{\phi_M}{\phi_i}}{\ln \frac{a}{b\phi_i} - 1} . \tag{11}$$

From step theory, for zero delay and $n = 1$, the maximum power is

$$\phi_M = \frac{\alpha^2}{2b} \quad . \tag{12}$$

Consequently, the maximum power during ramps is equal to that of steps having initial reciprocal period equal to the maximum reciprocal period of the ramps with a small correction factor which is the ratio of two logarithmic terms.

Results of the prompt approximation can now be discussed in somewhat more detail.

First, the power at the time of maximum reciprocal period is independent of the starting power and is determined solely by the reactivity addition rate, a, and the reactivity coefficient, b. The relation provides a determination of b from the ramp rate and the experimentally observed power at the time of maximum reciprocal period. The values of b thus obtained from ramp data were within a factor of two of the values obtained from the compensated reactivity and energy data from the series of step tests on each core.

The experimentally observed variation of power at maximum reciprocal period and reactivity coefficient, b, for the cores tested implies a relationship something less than the linear dependence predicted by Fuchs model ramp theory. Thus the modification to the theory, required to improve agreement with ramp data, is the same modification required for the step case; i. e., introduction of an nth order dependence of shutdown effects on energy to reduce the dependence on b.

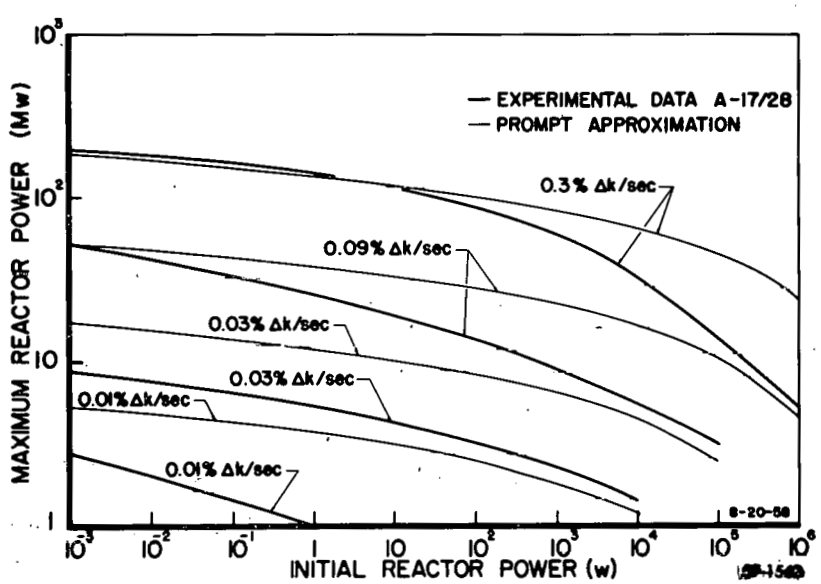

Fig. 18 - Maximum Power vs Initial Power - Prompt Model and Experimental Ramp Data

The results of Eqs. (5) and (8) are compared with experimental data in Fig. 18 where the maximum reactor power is plotted versus the initial power as functions of ramp rate. The experimental data are indicated by the heavy solid lines and are relatively insensitive to the starting power and more strongly dependent on ramp rate. The maximum power predicted for the various ramp rates is plotted as light lines and gives good agreement for the two highest ramp rates at the low starting powers. The hazards situation best represented by these tests is the startup accident.

In Fig. 19, the maximum reciprocal period from the prompt approximation is compared with experiment. The maximum reciprocal period is plotted versus starting power for the several ramp rates investigated with the A-17/28 core. The experimental data indicated by the solid line demonstrate a weak dependence of the maximum reciprocal period on the initial power and stronger dependence on ramp rate, a.

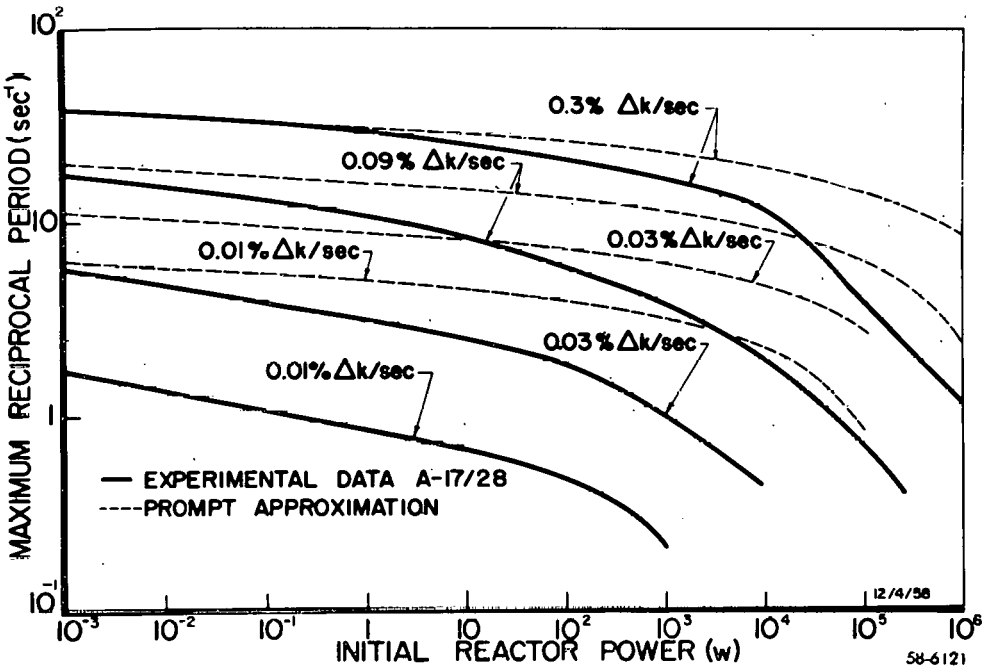

Fig. 19 - Maximum Reciprocal Period vs Initial Power - Prompt Model and Experimental Ramp Data

The values of maximum reciprocal period predicted by the prompt approximation are indicated by the dashed lines for each of the experimental ramp rates. The agreement is good for the 0.3% Δk/sec ramp rate, but becomes successively worse at the lower ramp rates. This lack of agreement is to be expected since delayed neutrons, which have been entirely neglected in the theory, are of greater importance on the slow ramps. Prompt critical is reached in a short time on fast ramps; consequently, a prompt approximation should yield results in agreement with experimental data. In all cases, the prompt approximation gives values of the maximum reciprocal period larger than those experimentally observed which, from a safety standpoint, enhances its usefulness.

The extension of the method to include delayed neutrons for the ramp case is done in the following way. Eq. (7) is used to compute the power at which the maximum k occurs. Then, assuming that the maximum α occurs at nearly the same power, the kinetics equations with delayed neutrons are used in any convenient way to compute the α of the system when the power has risen to the value given by Eq. (7), starting from a prescribed initial power. It is assumed that, similar to the prompt case, the shutdown term bE in Eq. (5) is small compared to the term at whenever the power is less than that given by Eq. (7).

An approximation due to Hurwitz[13] has been used in an unpublished work of Walker to incorporate the delayed neutron behavior into the model. The method also uses the assumption that shutdown effects are negligible up to the time of maximum reciprocal period, which is certainly valid for low starting powers. For high starting powers, it might be expected to be less satisfactory since shutdown effects appear earlier. However, agreement is still quite good, as may be seen in Fig. 20, in which the maximum reciprocal period is shown on the ordinate and initial power on the abscissa with ramp rate as the parameter. The experimental data from tests on the A-17/28 core are indicated with the heavy solid line and the predictions derived after inclusion of delayed neutrons by using the Hurwitz approximation are shown by the dashed lines. For all values of reactivity addition the agreement is good, especially at low starting powers. At the high starting powers some disagreement is to be expected since shutdown was neglected. A more accurate evaluation of the expressions leading to the maximum reciprocal period, utilizing machine calculations would be expected to produce closer agreement for the highest starting powers.

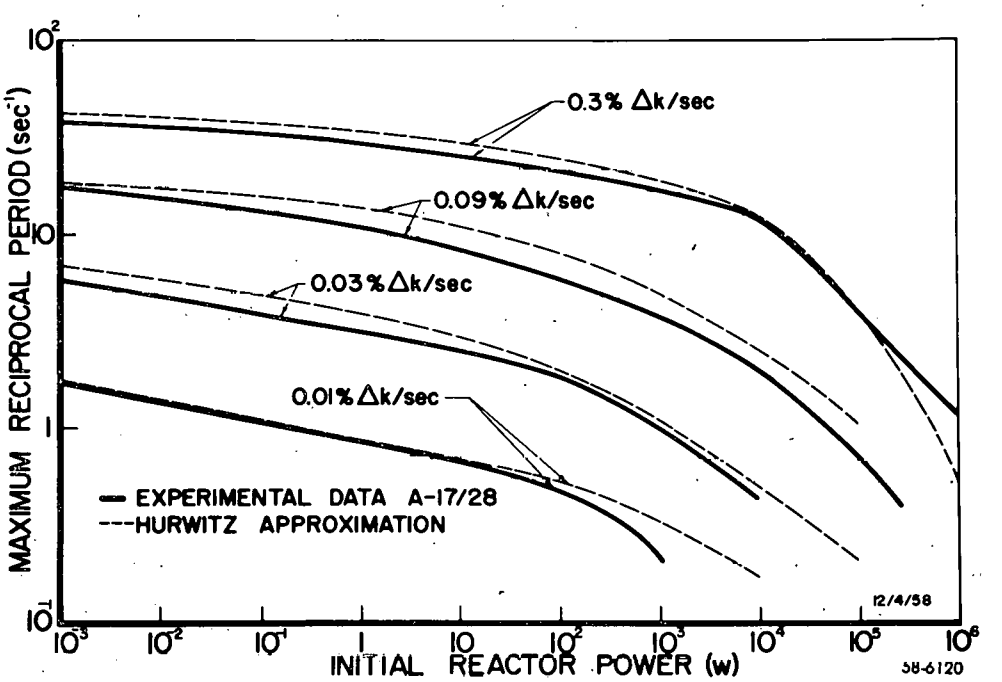

Fig. 20 - Maximum Reciprocal Period vs Initial Power - Model Including Delay Groups and Experimental Ramp Data

Three conditions can be established with these results and are indicated in Fig. 21. The straight line represents a condition that any ramp excursion, either prompt or less than prompt, can occur only for those values of initial power and ramp rate lying to the right of this line. This limit must be regarded as qualitative since an adequate description of the high power starting condition would necessarily include escape of shutdown energy, which is neglected in the model. The curved line represents the combination of conditions which result in a maximum $\alpha = 7$, which is approximately prompt critical for these Spert cores. The Spert step-transient data predict that significant core melting will occur for $\alpha > 250$. This value of α can be obtained on ramp excursions for combinations of conditions defined by the dashed line. Values to the left of the line are for excursions which will safely self-limit without melting.

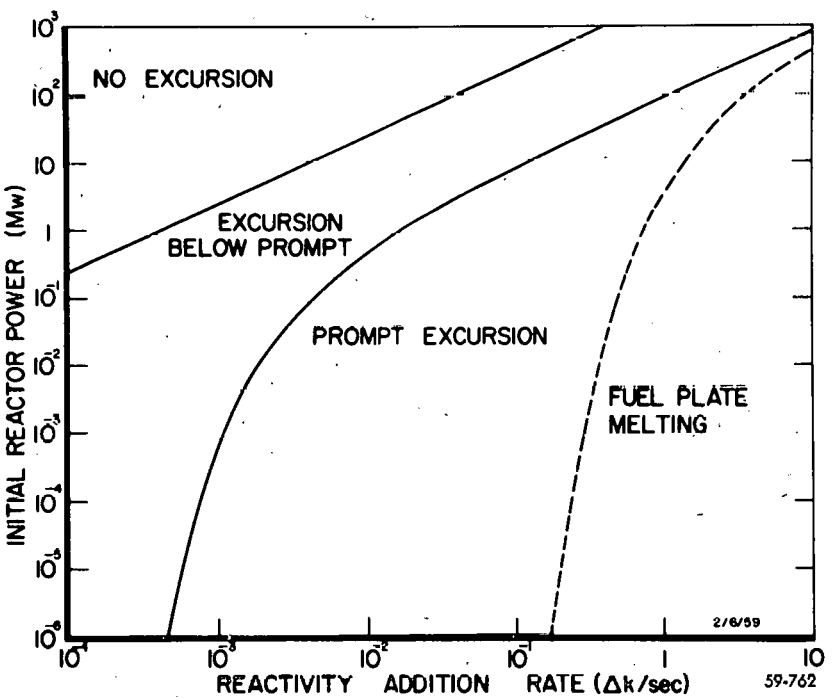

Fig. 21 - Conditions for Ramp Induced Excursion

In summarizing the transient behavior of these cores following a ramp addition of reactivity, the important results can be stated as follows: first, the most important parameter is the reactivity insertion rate, since it affects the transient behavior more strongly than either the initial power or the reactivity coefficient; second, the ramp and step excursions are equivalent in terms of maximum α; and finally, the simple elementary model employed to describe step tests also, properly modified, describes ramp tests and provides an analytical method of obtaining values of the maximum reciprocal period, and consequently, ramp behavior can be predicted from the results of step experiments.

Shutdown Processes in the Spert Reactor

The preceding sections have dealt with a general model for reactor kinetic behavior, and the experimental results were shown to be in satisfactory agreement with the theory. However, the mechanisms responsible for the self-limiting behavior were not discussed nor do they appear specifically in the theory. The identification of the constant, b, in the theory as the ratio of the void coefficient to the effective prompt neutron lifetime does not contribute significantly to the understanding of the mechanisms involved. If the experimental results are to be extrapolated to markedly different reactor systems, the processes must be identified. This section describes the work on detailed calculations of the reactivity effects from specific mechanisms.

The hypothesis of a radioactive prompt fission product having a large absorption cross section for thermal neutrons has been advanced as an explanation of reactor self-shutdown(14). Since no definitive experiments establishing physical bases for any explanations of self-limitation of power excursions have been performed, this model, like others, must be evaluated by considering plausibility of assumptions, correlation with data, and reasonability of the values of physical constants required to provide correlation with data(15). Several special cases have been considered.

In the first case, a detailed investigation was made to determine the conditions under which shutdown can occur from a short-lived, large cross section, prompt fission product. The investigation was carried out using step reactivity inputs and a prompt, one-group model, which should yield all the general features of this type of shutdown. If rate of poison density generation is characterized as a constant times the neutron density, it is found that shutdown can occur only for initial reciprocal periods less than this constant. Further investigation of this case shows that shutdown from a long half-life poison will result in a single power peak, whereas a sufficiently short half-life can cause damped oscillations in the power for certain initial periods.

All the burst shapes predicted by this first model show a much slower power fall-off after peak than has been observed in the Spert experiments, so a modification was introduced to obtain a better fit in this region. For this case the poison is hypothesized to be an intermediate member of a decay sequence rather than a direct fission product, and a better description of post-peak behavior is obtained.

In both cases, the form of the pertinent equations is reasonable and the general behavior of their solutions agrees with observed reactor behavior. The poison has not been observed directly; therefore, the correlation between the behavior predicted by the model and the experimental data cannot be construed as positive evidence for its validity because the equations are quite similar to those describing any model in which shutdown effect is proportional to energy release.

A lower limit for the required poison cross section of 6×10^{10} barns is obtained from experimental values of energy release and reactivity compensation observed for reactor transients. An upper limit for its half-life of 3 sec is obtained by noting the elapsed time between a power peak and the minimum after the peak. This cross section is much larger than the present theoretical limit, given by the Breit-Wigner formula, of about 10^8 barns, and also much greater than the largest observed value of 3×10^6 barns for Xe^{135}.

Since the required cross section is unreasonably large and the equations are essentially those of a simple energy shutdown model, it is concluded that the poison model affords no advantages over other, more reasonable, explanations of reactor self-shutdown.

Among these other possibilities are thermal processes(16). In the step transient tests it has been observed that, for bursts having initial asymptotic periods of less than about 50 msec, the fuel plate surface temperatures exceed the boiling point of water before peak power is reached. Thus, for these tests, boiling would be expected to contribute to the self-shutdown process. However, the formation of steam voids under transient conditions is not sufficiently well understood to permit exact calculations of void growth during a burst. The reactivity changes observed under these conditions indicate clearly that the steam volume is at least an order of magnitude less than would be predicted on the basis of steady state heat transfer.

A number of possible explanations exist, such as suppression of the boiling point by transient pressures, steam blanketing of the fuel plates, and requirements for transient superheats to initiate boiling. Analyses based on these various hypotheses have been tried by several authors, and in every case, some degree of success has been achieved in matching the Borax data in the short period region. In this discussion an alternative approach is introduced which correlates a somewhat wider range of data than previous treatments.

It is generally agreed that the high heat transfer rates observed in sub-cooled nucleate boiling are a result of bubble agitation of the boundary layer, with only a small fraction of the energy transported by the bubbles themselves(17). If it is assumed that under transient heating conditions this "micro-convection" will not develop instantaneously, the transient heat transfer rates may be treated as characteristic of conduction to stagnant water rather than of boiling. The temperature distribution in the moderator may then be calculated by a simple thermal diffusion equation. If it is also assumed that a fixed fraction of the transferred heat goes into steam formation, the steam void growth can be calculated and the behavior of the reactor thereby predicted. This approach has been used in the analysis and is referred to as the Conduction Boiling Model.

Analytical expressions have been obtained for the reactor power, energy released, and fuel plate temperature at the peak of the power burst as functions of the reactor period and of the initial temperature.

The fraction of energy going into steam formation is treated as an arbitrary constant, the value of which is adjusted to give the best fit for a given series of experiments. The analytical results have been compared with experimental data from four Spert I cores and Borax I at initial temperatures of 20°C and at boiling.

These comparisons are shown in Figs. 22 through 26. Fig. 22 compares the predicted behavior of the Spert I A core with experimental results for both boiling (95°C) and 20°C initial temperatures. The peak power, the plate temperature at the time of peak power, and the energy release up to the time of peak power, referred to the scale at the left in arbitrary units, are plotted versus the reciprocal of the initial asymptotic period, α, given in sec^{-1} on the lower scales. The solid lines represent the values of these quantities predicted on the basis of a given fraction of the energy transferred to the water at above-boiling fuel plate temperatures going into the formation of steam. The quantity of steam for each case is equated to the void size required for the proper reactivity compensation at peak power. In order to obtain values for the energy release, peak power, and plate temperature rise, a power-time behavior of a simple exponential form has been assumed. This form does not correspond to the actual time behavior of the reactors, but is applicable because of the constant power burst shape exhibited by the reactors investigated for transients in which boiling temperatures are exceeded.

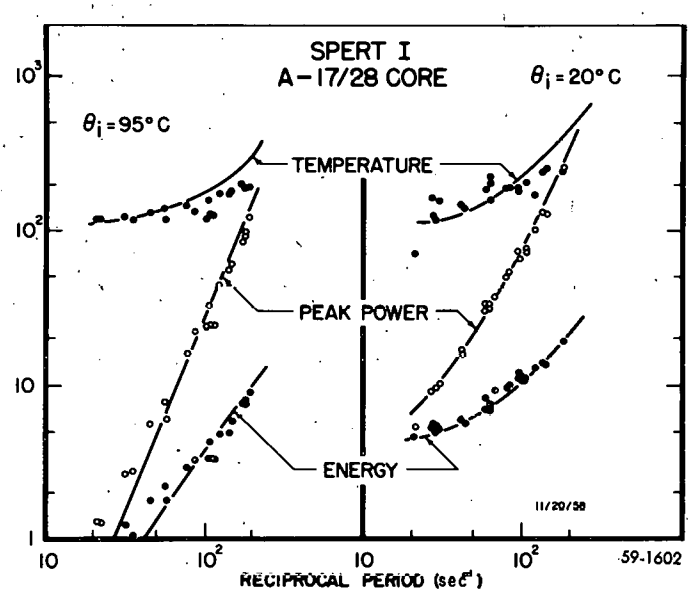

Fig. 22 - Comparison of Conduction Boiling Model with Experimental Data

The figure shows the excellent agreement between these predicted quantities for the Spert I A core, and the experimental values as shown by the circles for both boiling and ambient initial temperatures. The initial temperatures are given at the top of each graph.

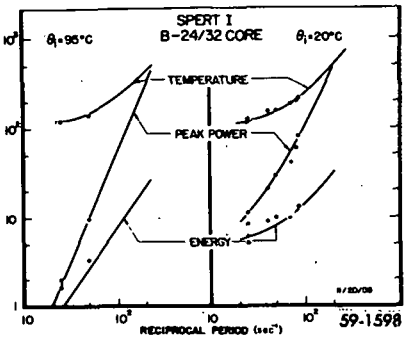

Fig. 23

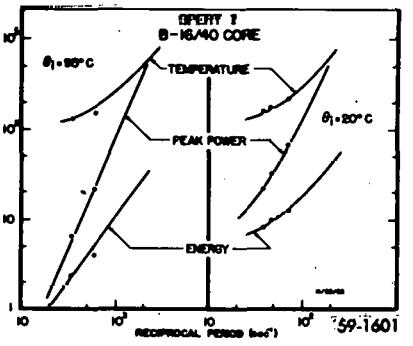

Fig. 24

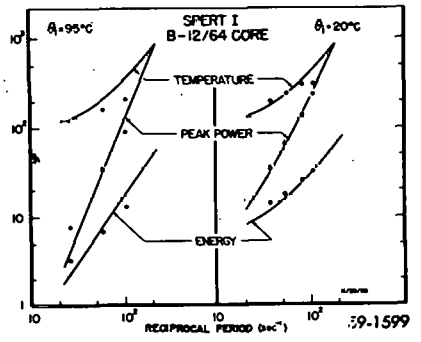

Fig. 25

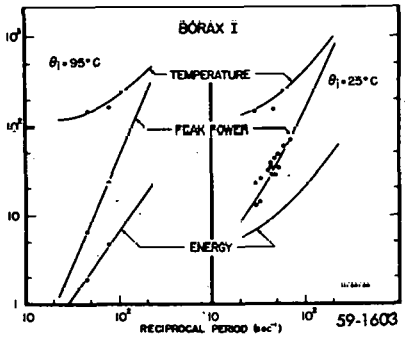

Fig. 26

Figs. 23 - 26 - Comparison of Conduction Boiling Model with Experimental Data.

Figs. 23, 24 and 25 show the same comparisons for the B-24, B-16 and B-12 cores and again show the same good correlation. It is noteworthy that this simple shutdown theory applies so successfully to all three B cores used in the Spert I reactor, since these cores cover a large range of practical designs for swimming-pool type reactors.

Fig. 26 shows the results of this model as applied to Borax I. While experimental data are not available for all curves, good agreement with the calculations exists where the comparison can be made.

Although the Conduction Boiling Model provides quite satisfactory agreement with the experimental data, the assumptions, while reasonable, are rather arbitrary in nature and probably represent an over-simplification of the actual physical processes involved. The empirical agreement obtained should not be construed as establishing the validity of the assumptions contained in the theory.

In the longer period region, where boiling can not contribute to shutdown, an investigation has been made into the effects of thermal expansion of the core and moderator on reactor shutdown. The shutdown mechanisms which are considered here are those based on either conductive heat transfer or direct neutron, gamma ray and fission heating. The resultant physical changes which produce reactivity effects are the following: reduction in moderator density due to thermal expansion of the moderator, moderator expulsion resulting from thermal expansion of the metallic core structure, and core geometry changes associated with the heating of the mechanical structure.

The power burst is approximated by the two-term form

$$\phi = \phi_0 \left[re^{\alpha t} - (r - 1)\, e^{\frac{r}{(r-1)}\alpha t} \right] \qquad (13)$$

where ϕ_0 is the peak power, α is the reciprocal of the initial asymptotic period, t is the time as measured from peak power, and r is a fitting constant.

In Fig. 27 a representative power burst, indicated by circles, is compared with this two-term exponential representation, indicated by the solid line. The fitting parameter, r, can be found geometrically by extending the asymptote to the leading edge of the power burst to the time of peak power. Its magnitude is the ratio of this asymptote at the time of peak power to the peak power value. This asymptote is simply the first term of the exponential representation, hence α may be found from its slope.

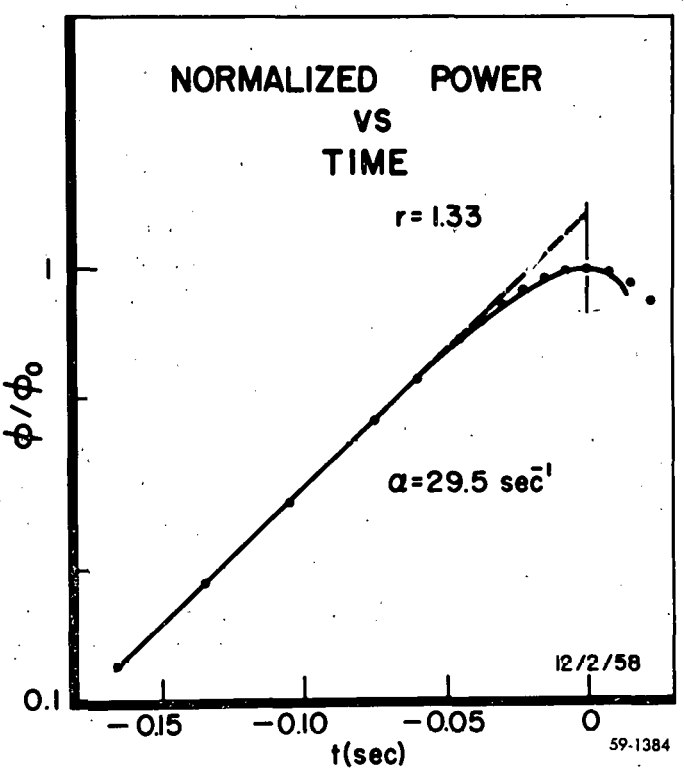

Fig. 27

The agreement between the experimental burst shapes and the two-term representation for α greater than five is good enough so that negligible errors arise from its use in heat transfer calculations. For α less than five, it is necessary to introduce artificial values of α into the two-term form to obtain suitable representations of the burst shapes. With this modification accurate calculations can be made over the entire α range covered by experiment. Since the heat transfer processes under consideration can be treated as linear, the use of this burst shape allows analytic solutions of the reactor temperature distributions, which then permit the inclusion of non-linear effects, such as thermal expansion of the moderator, to be treated in a straightforward manner.

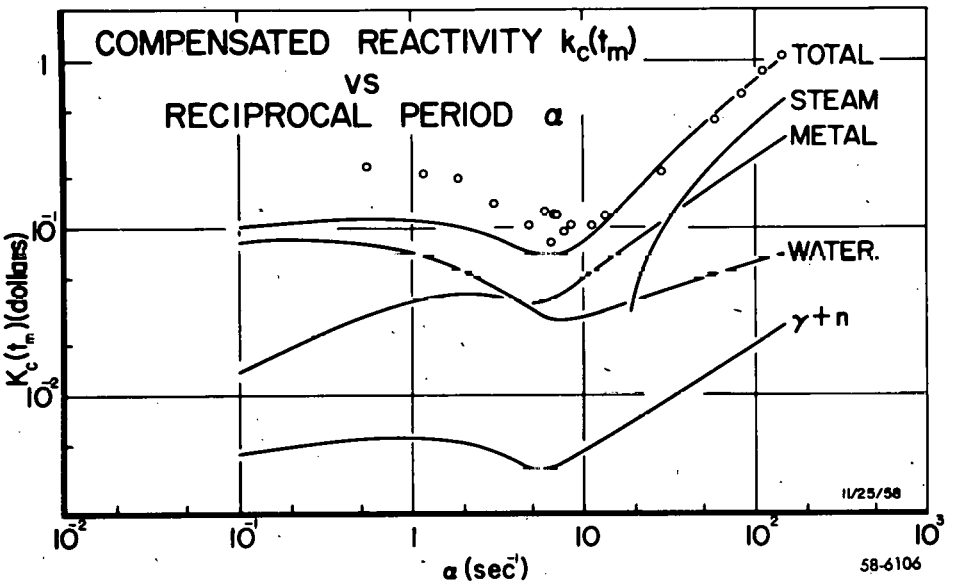

Fig. 28

Fig. 28 shows the compensated reactivities at the time of peak power versus α for the Spert I A core with initial temperatures of 20°C. The lower solid curve is the contribution due to direct gamma and neutron heating of the moderator, and is linear with energy release. The curve labeled "water" represents the loss in reactivity due to expansion of the water moderator from conduction heating and includes the non-linear expansion characteristics of water. For very small α this contribution is responsible for the bulk of the known shutdown effect due to the relatively high temperature coefficient of expansion of water. For large values of α, however, the power bursts are of such short duration that little heat is transferred to the moderator, so that this term contributes only slightly to the shutdown.

The curve shown for the metal expansion contribution includes the effects of both moderator expulsion from the core and reactor geometry changes. It is interesting from a safety standpoint that this contribution is quite sizable in the region of large α, for if all other shutdown effects were absent, the metal expansion alone would limit energy releases to safe levels for α as large as 50.

The sum of these three contributions, plus a steam term taken from the Conduction Boiling Model, form the "total" compensated reactivity curve which can be compared directly with the experimental values indicated by the circles. It should be noted that the total compensated reactivity curve has a shape quite similar to the energy release up to the time of peak power, which is proportional to the lower curve. The

similarity of the α-dependence of these two functions is undoubtedly responsible for the success of simple energy shutdown models in the prediction of reactor self-limiting behavior.

Comparing the calculated total compensated reactivity curve with the measured values over the entire range of experimental data available, it is seen that the agreement is generally very good. There is one region, in the neighborhood of $\alpha = 1$, where the calculated value falls somewhat short of accounting for the entire reactivity change. In this region radiolytic gas is expected to contribute to the shutdown, but no calculations of its effect have been made due to the lack of an adequate description of the evolution of this gas under transient conditions.

In the region from $\alpha = 5$ to $\alpha = 20$, the known effects account for the entire reactor shutdown within the limits of calculational errors, which here are about $\pm$ 15 per cent. This complete shutdown description by well-understood mechanisms is of considerable aid in establishing upper limits to contributions from postulated shutdown models such as the Poison Model presented earlier.

For α greater than 20, the inclusion of the steam shutdown term gives a very good fit between the calculated and measured compensated reactivities. Here the steam contribution has been adjusted at $\alpha = 100$ to fit the difference between a measured compensated reactivity and that calculated from known effects. The exactness of this fit is important from a reactor safety standpoint, since a single experimental determination of the steam fraction mentioned in the Conduction Boiling theory allows an accurate prediction of the transient characteristics of a given reactor over the entire large α region. With such a technique available, it may be unnecessary to carry out extensive experiments in the potentially dangerous large α region to locate important safety parameters, such as the α associated with fuel-plate melting.

In summary, it appears that satisfactory descriptions of reactor shutdown behavior have been obtained over the regions most important from a safety standpoint. The calculations of the known thermal effects are easily made and could be used alone to find somewhat conservative limits on transient operation. However, the inclusion of shutdown effects from the Conduction Boiling Model gives very good predictions of behavior over the entire large α region, with only a single experimental determination needed for its use.

Since this model is empirical, the agreement between calculations and experimental data does not imply verification of the model. Thus, other mechanisms such as radiolytic gas formation[3], cannot be excluded as possible contributers to the observed shutdown effects.

REFERENCES

1. S. G. Forbes, Trans. Am. Nuclear Soc. 1 (2), 84 (1958).

   J. E. Grund, Trans. Am. Nuclear Soc. 1 (2), 84-86 (1958).

   F. L. Bentzen, W. E. Nyer, Trans. Am. Nuclear Soc. 1 (2), 86 (1958).

   J. C. Haire, W. E. Nyer, Trans. Am. Nuclear Soc. 1 (2), 86-87 (1958).

   R. F. Walker, P. French, S. G. Forbes, Trans. Am. Nuclear Soc. 1 (2), 87-89 (1958).

2. W. E. Nyer, S. G. Forbes, F. L. Bentzen, G. O. Bright, F. Schroeder, and T. R. Wilson, "Experimental Investigations of Reactor Transients", IDO-16285 (April 20, 1956).

3. F. Schroeder, S. G. Forbes, W. E. Nyer, F. L. Bentzen and G. O. Bright, Nuclear Science and Engineering 2, 96-115 (1957).

4. K. Fuchs, "Efficiency for Very Slow Assembly", LA-596 (August 2, 1946).

5. G. O. Bright, S. G. Forbes, W. E. Nyer and F. Schroeder, "An Elementary Model for Reactor Burst Behavior", IDO-16393 (August 2, 1957).

6. G. W. Griffing and L. I. Deverall, "Kinetic Studies of the Spert I Reactor, I - Initial Behavior by the Energy Model", IDO-16397 (April 18, 1958).

7. R. W. Miller, "Quarterly Progress Report, Reactor Projects Branch", April, May, June 1958, G. O. Bright ed., IDO-16489, 88-96 (January 19, 1959).

8. S. G. Forbes, "Quarterly Progress Report, Reactor Projects Branch", January, February, March 1959, J. A. Norberg ed., (to be published).

9. S. G. Forbes, "Quarterly Progress Report, Reactor Projects Branch", January, February, March 1958, G. O. Bright ed., IDO-16452, 38-64 (August 5, 1958).

10. R. W. Miller, "Calculations of Reactivity Behavior During Spert I Transients", IDO-16317 (June 1, 1957).

11. Detailed discussions of the static measurements may be found in the following publications:

    W. E. Nyer, et. al., op. cit.

    "Quarterly Progress Report, Reactor Projects Branch", July, August, September, 1957, G. O. Bright ed., IDO-16416 (October 1, 1957).

    "Quarterly Progress Report, Reactor Projects Branch", October, November, December 1957, G. O. Bright ed., IDO-16437 (March 21, 1957).

"Quarterly Progress Report, Reactor Projects Branch", January, February, March 1958, G. O. Bright ed., IDO-16452 (August 5, 1958).

12. W. E. Nyer, "Quarterly Progress Report, Reactor Projects Branch", January, February, March 1958, G. O. Bright ed., IDO-16452, 65-70 (August 5, 1958).

13. H. Hurwitz, Jr., "On the Derivation and Integration of the Pile-Kinetic Equations", AECD-2438 (April, 1948).

14. E. T. Clarke, "Initial Shut Off in a Spert I Type Reactor Transient", American Nuclear Society Abstracts, 23, (June, 1957).

15. R. F. Walker, "Quarterly Progress Report, Reactor Projects Branch", April, May, June 1958, G. O. Bright ed., IDO-16489, 96-110 (January 19, 1959).

16. Detailed discussions of thermal shutdown effects are available in the following publications:

"Quarterly Progress Report, Reactor Projects Branch", January, February, March 1958, G. O. Bright ed., IDO-16452 (August 5, 1958).

"Quarterly Progress Report, Reactor Projects Branch", April, May, June 1958, G. O. Bright ed., IDO-16489 (January 19, 1959).

"Quarterly Progress Report, Reactor Projects Branch", July, August, September 1958, G. O. Bright ed., IDO-16512 (May 6, 1959).

17. W. M. Rohsenow and J. A. Clark, Trans. ASME 73, 609-620 (1951).

18. W. E. Nyer and S. G. Forbes, Sec. Intern. Conf. Peaceful Uses Atomic Energy, Geneva 15/P/2428 (1958).

Phillips 66